*Plasma Chemistry and Plasma Processing, Vol. 25, No. 4, August 2005 (© 2005)*
DOI: 10.1007/s11090-004-3135-6

# Elimination of Carbon Monoxide in the Gas Streams by Dielectric Barrier Discharge Systems with Mn Catalyst

Chung-Liang Chang,[1,2] and Tser-Sheng Lin[1]

*Received October 4, 2004; revised December 2, 2004*

*Elimination of CO in air stream using the plasma catalytic reactors was investigated. Two plasma catalytic systems were evaluated in this study, one consisting of a catalyst-bed packed in plasma zone of a dielectric barrier discharge (DBD) reactor directly (CID reactor), and the other (CAD reactor) consisting of a catalyst-bed after a DBD reactor. The examined operating parameters in this study included applied voltage, discharge power, the lengths of plasma zone and catalyst-bed, and inlet CO concentration. It was found that the glass packed DBD reactor without catalyst cannot eliminate CO in air stream effectively. When $MnO_x$ catalyst applied to DBD reactors, the removal of 1000 ppm CO can achieve to 97% by both type reactors. Under constant energy input condition, the CO removal of a CID reactor increased with the decrease of the initial CO concentration and the increase of the length of catalyst beds. In addition, the operating energy consumption of CID system was lower than that of CAD system.*

**KEY WORDS:** Dielectric barrier discharges; carbon monoxide; Mn catalyst; air pollution control technology; nonthermal plasmas.

## 1. INTRODUCTION

The dielectric barrier discharge (DBD) system, a popular nonthermal plasma (NTP) technique, operating at near normal atmospheric pressure and temperature has been successfully applied to commercial ozone generators.(1) And its potential application in removing various air pollutants such as volatile organic compounds (VOCs), nitrogen oxides and sulfur oxides has been studied.(2–4) The utilization of NTP can make more VOCs to be decomposed; but, unfortunately, the carbons of VOCs cannot be oxidized to $CO_2$ completely during the plasma decomposition processes. The conversion of carbon atoms to $CO_2$ is only between 30% and 65%

[1]Department of Environmental Engineering and Health, Yuanpei Institute of Science and Technology, Hsinchu, Taiwan.
[2]To whom correspondence should be addressed. E-mail: clchang@mail.yust.edu.tw

and thus a large amount of CO is released.[5] Furthermore, the increase of background oxygen level cannot effectively reduce CO formation; for instance, the ratio of $CO/(CO + CO_2)$ was around 70% in the effluent when the $BaTiO_3$ packed-bed DBD reactor was utilized to destruct $CH_3Br$.[6] In addition, Malik and Jiang[7] found that the increase of inlet toluene and benzene concentrations led to more CO formation. The maximum ratios of $CO/CO_2$ observed in their study were 2.5 and 3.0 with respect to toluene and benzene.

In order to improve the performance of plasma system on VOCs decomposition, catalyst beds were applied in the NTP reactors. Two types of the DBD reactors combined with catalyst beds have been designed: (a) CID reactor: catalytic material packed into the plasma zone of DBD reactors directly; (b) CAD reactor: catalytic materials packed after DBD reactors rather than in the plasma zone of these reactors. In fact, many catalysts, such as $Al_2O_3$,[7] $Ag/TiO_2$,[8] $Pt/Al_2O_3$[9,10] and $LaCoO_3$ catalyst,[5] have been placed in plasma reactors in order to enhance VOCs decomposition and to decrease CO formation.

In addition, ozone may be introduced into contaminated gas streams before they are passed over a catalyst-bed in a CAD reactor to allow a low-temperature catalytic oxidation reaction occur. This process utilizes the oxidizing power of ozone together with the activity and selectivity of oxidation catalysts to convert carbon monoxide and VOCs to $CO_2$. Because of the usage of ozone, the heating of air stream is not required.[11] The CAD process is sometimes called as "ozone catalytic oxidation technology". The utilization the $MnO_2$, Ni, Cu, and Ni–Cu catalyst in a DBD reactor downstream can promote benzene and toluene decomposition.[12,13] With regards to the reactions of ozone decomposition and CO oxidation by ozone on catalysts, the $Au/Fe_2O_3$,[14] $CeO_2$,[15] Mnx catalysts[16] have been investigated. Naydenov *et al.*[15] pointed out that the oxidant in the low-temperature oxidation of CO was highly reactive atomic oxygen, which was produced by ozone decomposition on the oxide surface. Mehandjiev *et al.*[16] suggested that the catalytic ozone oxidation followed the Eley–Rideal mechanism.

These studies clearly pointed out that the CID and CAD reactors with different catalysts could reduce CO emission from gas streams. Unfortunately, the experimental operation conditions were different in these individual systems. Therefore, it is very difficult to determine which type of reactor is better based on the available data. This study intends to compare the removal efficiency of CO in CAD and CID reactors with $MnO_x$ catalytic material packing. In addition, the ozone decompositions in both reactors were evaluated in the present study as well.

## 2. EXPERIMENTAL

A schematic diagram of the experimental system is illustrated in Fig. 1. The dry-grade compressed CO (10% CO in pure $N_2$) and air (80% $N_2$ and 20% $O_2$) cylinders were used to supply CO and air streams. The flow rates of all air streams were regulated by mass flow controllers (Brooks, 5850). The base line operation conditions as followed: (1) the initial concentration of CO: 1000 ppm and (2) the overall operating flow rate: 1000 mL/min.

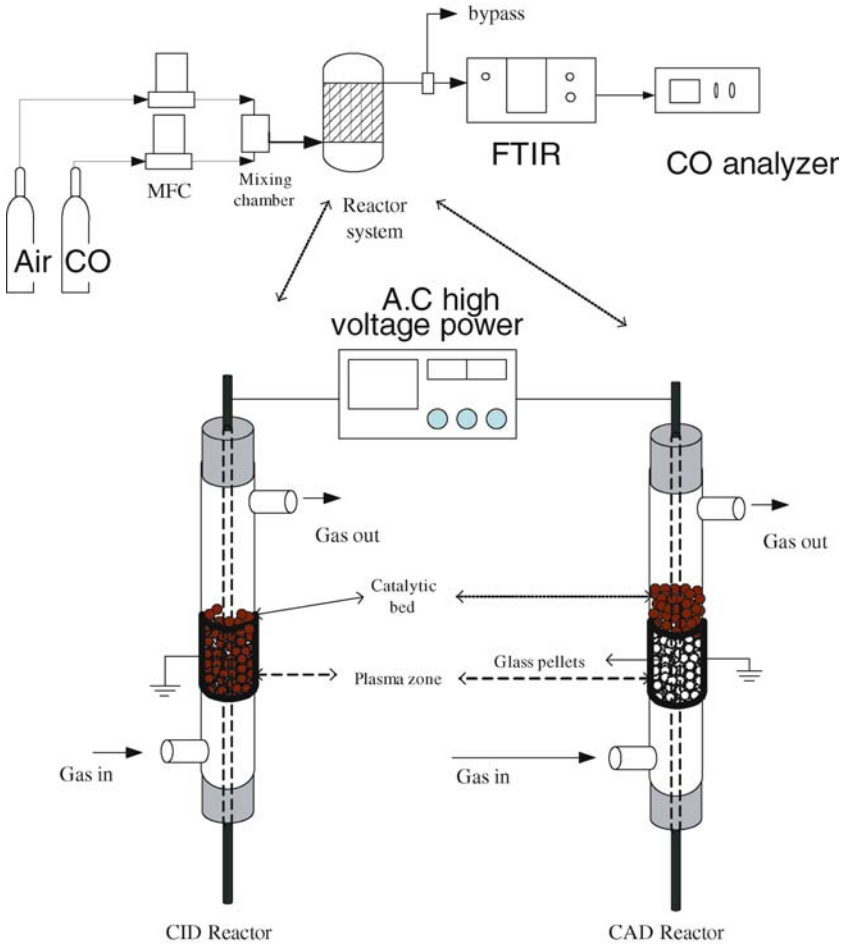


**Fig. 1.** Schematic of the experimental apparatus.

Two types of reactors, CAD and CID reactors, were used for testing. For CAD reactor tests, the 5 mm nonporous glass pellets were placed inside the wire-tube DBD plasma reactor (glass/DBD reactor) between two electrodes to generate ozone. This DBD reactor was composed of a Pyrex-glass tube (I.D.: 20.0 mm) and a stainless steel wire (5.0 mm diameter) that was suspended along the axis of the tube and served as an inner electrode. The outer electrode (ground electrode) was made of stainless steel wire mesh and was wrapped around the outside of the glass tube. High voltage power was applied to the inner electrodes to generate plasma. After the ozone generation zone, the system connected to the various lengths of $MnO_x$ catalyst beds for testing.

For CID reactor tests, a reactor with the same geometric described earlier was used. The major difference between CAD and CID reactors was that the CID reactor utilized the Mn catalytic pellets instead of glass pellets placed inside the plasma region between two electrodes. In addition, the various lengths of ground electrodes could charge the plasma zone. The plasma zone was fixed while the length of Mn catalyst beds was varied in this study. In this case study, the operating flow rate was 1000 mL/min, the actual average residence time per unit length of packed reactors was 0.025 s/cm. The temperature of both reactors was maintained at room temperature (approximately 25 °C) by a cooling fan.

The impregnation method was utilized to prepare $MnO_x$ catalytic pellets. $Al_2O_3$ pellets purchased from K.J. Environmental Technology Co. Ltd. (Taiwan) as metal support were impregnated with an aqueous solution of $Mn(NO_3)_2{\cdot}4H_2O$ (analytical grade, Merck). The diameter of $Al_2O_3$ pellets was 5 mm. The $Al_2O_3$ pellets and impregnating aqueous solution were placed in a custom-made furnace equipped with a rotary device for 12 h under the following conditions: (1) rotation speed: 5 rpm; (2) temperature: 120 °C. Then, the impregnated pellets were calcined in air at 600 °C for 8 h. The content of Mn metal on the $Al_2O_3$ pellets was quantified by an atomic absorption spectrometer (Hitachi Z8100) followed by dissolving these oxides of metals with a hydrofluoric acid solution. The content of Mn metal on $Al_2O_3$ pellets was 0.25 wt% in this study. The surface areas of the packing pellets were measured using a Micromeritics ASAP2000 device. The surface areas of $Al_2O_3$, and Mn coated pellets were 293 and 187 $m^2/g$, respectively.

A Testo535 on-line analyzer was used to measure the CO concentrations in the outlet airflows. Ozone concentration in the outlet gas flows was analyzed by a Fourier transformation infrared spectrometer equipped with a gas cell (FTIR, BRUKER, VECTOR 22, Infrared Analysis Inc., model 2.4-P. A.). The sampling streamline was passed through the FTIR gas cell and then was introduced to the CO analyzer at a flow rate of 500 mL/min. The removal efficiency of CO is defined as

$$\eta = \frac{CO_{in} - CO_{out}}{CO_{in}} \times 100\%$$

where $CO_{in}$ and $CO_{out}$ are the inlet concentration and the outlet concentration of CO, respectively.

The 60 Hz AC power was applied to the inner electrode. The voltage applied to the plasma reactor was controlled from 11 to 19 kV to change the discharge power. The high voltage and current input to the corona reactor were monitored and measured by a Tektronix digital oscilloscope (Model TDS-340A). A Tektronix P6015 HV probe was employed to reduce the high voltage signal before it was fed to the oscilloscope. A current probe (Tektronix, Model A6302 and AM503B) was used to measure the current during corona discharge. The actual discharge power input to the reactor system was determined by the product of the voltage and current. Figure 2 shows the relation of applied voltage to discharge power over glass/DBD reactors and CID reactors with different length of plasma zone. As seen, the input power showed an increasing trend as applied voltage and plasma length. The $MnO_x$ catalyst packing could lead a greater discharge power compared with glass packing in the same geometric DBD reactor at same applied voltage.

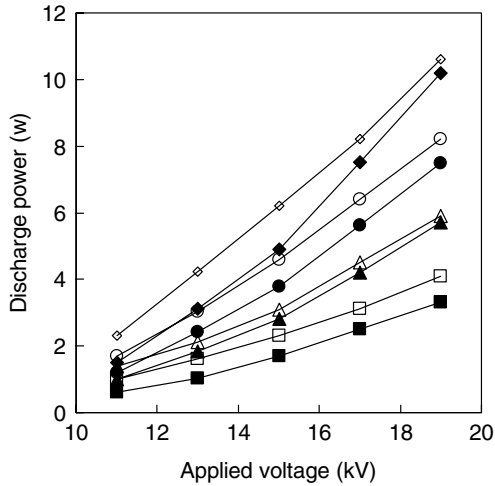


**Fig. 2.** Discharge power of glass/DBD reactor and CID reactors with different lengths of plasma zone as a function of applied voltage. Solid symbol: glass/DBD reactor. Open symbol: CID reactor. ■, □: 4 cm; ▲, △: 7 cm; ●, ○: 10 cm; ♦, ◇: 13.7 cm.

## 3. RESULTS AND DISCUSSION

The influence of applied voltage on the ozone concentration produced by different lengths of glass/DBD reactors with/without CO is shown in Fig. 3. The formation of ozone increases as the lengths of plasma zone (glass packed-bed) and applied voltage increases. The maximum ozone concentration observed was 2235 ppm in a 137 mm glass/DBD reactor at an and applied voltage of 19 kV. The results also show that the existence of CO in air could not influence on the ozone production in glass/DBD reactors and the ozone concentration remained at the similar value observed under the air only condition. In addition, Fig. 4 shows that the CO could not be removed from gas streams by simply passing them through the DBD reactor. It is due to that CO is more difficultly ionized than $O_2$ in the glass/DBD process because of the ionization potential of CO is 14 eV, which is higher than that of $O_2$ (12 eV). Thus, plasma energy of glass/DBD reactors would react with $O_2$ to form $O_3$ rather than CO. The results also imply that the higher ozone concentration could be produced in the gas stream; however, CO is quite stable and cannot be oxidized by $O_3$ in gaseous phase.

When the $MnO_x$ coated pellets were utilized as packed-bed placed after the plasma zone of CAD reactors, the removal of CO with an initial concentration of 1000 ppm is displayed in Fig. 4. In this case study, the operating flow rate was 1000 mL/min, the length of the catalyst-bed

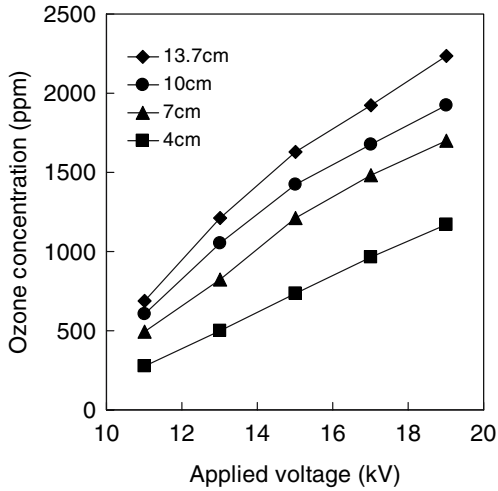


**Fig. 3.** The influence of applied voltage on the ozone productions for different lengths of glass/DBD reactors with/without CO.

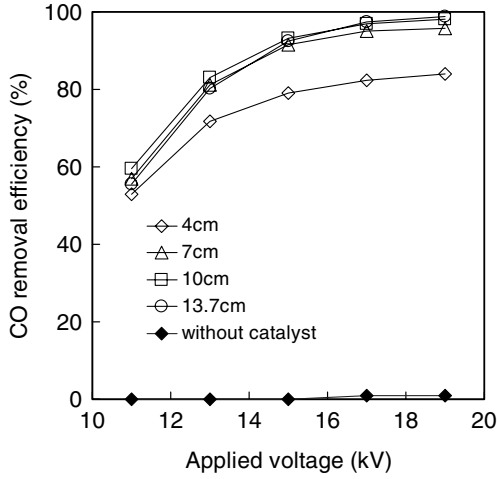


**Fig. 4.** CO removal efficiency of glass/DBD reactor without catalysts and CAD reactor with different lengths of catalyst-bed.

was set to 4, 7, 10 or 13.7 cm that corresponded to an actual average residence time of 0.21, 0.37, 0.53, and 0.72 s, respectively. In addition, the length of glass/DBD reactor was fixed at 13.7 cm to produce ozone. The best removal efficiency of the 4 cm $MnO_x$ packed-bed reactor was 84% at the applied voltage of 19 kV on a glass/DBD reactor. When the length of $MnO_x$ packed-bed was increased to 7 cm, the best CO removal efficiency observed could reach to 96% under the same operation conditions. However, the results shown in Fig. 4 exhibit that when the length of $MnO_x$ catalyst-bed is longer than 7 cm, the CO removal efficiency seems not be increased any more.

The ozone concentrations in the effluents from CAD reactors as function of applied voltage are shown in Fig. 5. When the ozonized gases passed through the $MnO_x$ packed-bed reactors, the ozone concentration could be significantly reduced. In addition, the ozone decomposition efficiency increased as the length of packed-bed increased. In the case of the applied voltage of 19 kV on the glass/DBD reactor, the inlet ozone concentration was approximately 2235 ppm (Fig. 3), and the ozone concentrations in the effluents from 4 to 7 cm $MnO_x$ catalyst beds were 456 and 63 ppm, which corresponded to 80% and 97% decomposition. In addition, the rate of ozone decomposition corresponding to the above two cases were $3 \times 10^{-3}$ and $2 \times 10^{-3}$ mol/min/g greater than that reported for the $MnO_2/\gamma\text{-}Al_2O_3$, which ranged from $6 \times 10^{-5}$ to $8 \times 10^{-5}$ mol/min/g.[17]

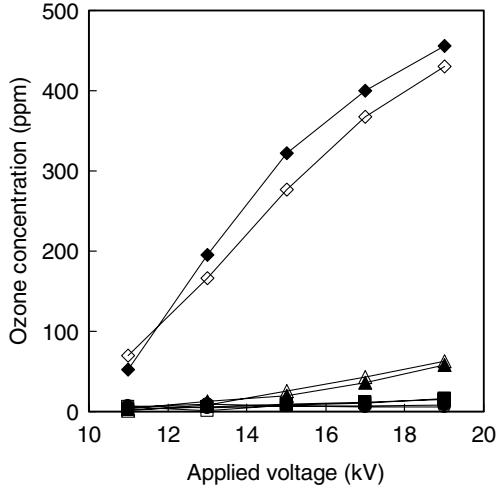


**Fig. 5.** Ozone concentration effluents from CAD reactor with different lengths of catalyst-bed. Solid symbol: air without CO. Open symbol: contain 1000 ppm CO. ■, □: 4 cm; ▲, △: 7 cm; ●, ○: 10 cm; ♦, ◇: 13.7 cm.

When the length of catalyst-bed was extended up to 10 or 13.7 cm, the decomposition efficiencies almost achieve 100%. It is noteworthy that the effect of CO existence in air stream on ozone decomposition by $MnO_x$ catalysts was not significant. The results shown in Figs. 4 and 5 suggest that the CO can react with O active species on the catalytic metal surface to form $CO_2$. The total amounts of ozone decomposition were 1.4–2.5 times greater than that of CO removal. In addition, ozone was almost decomposed completely if the catalyst-bed was longer than 7 cm that resulted in no active species remained on the later catalyst surface to oxidize CO. Thus, the CO removal by CAD was limited by availability of ozone and could not further be increased with the length of catalyst beds.

When glass pellets were replaced by $MnO_x$ coated pellets as packing in the plasma reactor for CID system, the influence of applied voltage on the CO removal efficiency is shown in Fig. 6. As shown, the CID system was also a good device for CO elimination. The increase of either the applied voltage or the length of $MnO_x$ catalyst-bed would lead to an increase of CO removal from air streams. The 13.7 cm $MnO_x$ catalytic CID reactor would eliminate CO completely at an applied voltage of 19 kV. In addition, we also evaluated the activity of $MnO_x$ during thermal oxidation process. The result shows that 1000 ppm CO in air stream at a flow rate of 1000 mL/min only 13.0% could be eliminated by $MnO_x$ coated

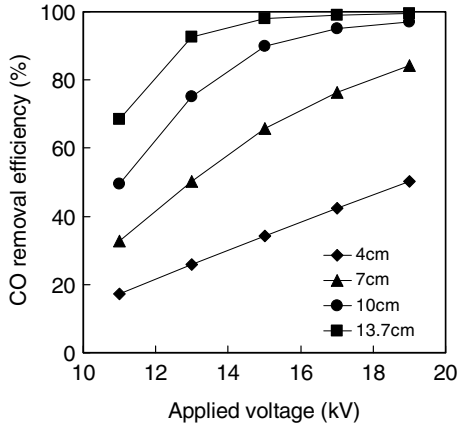


**Fig. 6.** CO removal efficiency of CID reactor with different lengths of catalyst-bed.

catalyst at 300 °C. Thus, both catalytic plasma processes are better methods to remove CO at lower temperature.

The ozone concentrations in the effluents from different lengths of CID reactors as function of applied voltage are shown in Fig. 7. The ozone concentration was increased with the increase of applied voltage. As compared with ozone released from glass/DBD reactors (Fig. 3), the ozone concentration in the effluents from CID reactor could be significantly reduced at the same applied voltage. Figure 7 shows that the ozone generation by our CID reactor was not significantly affected by the existence of CO. Figure 8 shows that the $MnO_x$ coated pellets placed in the plasma zone as compared with glass/DBD can lead ozone reduction of 80% to 91% at the same applied voltage. The results indicate that the amount of ozone produced in the gaseous phase in the plasma zone and they decomposed on $MnO_x$ catalyst to form O active species consequently. And the CO could react with O active species on the catalytic metal surface to form $CO_2$. This phenomenon suggests that the active species which resulted from ozone decomposition on the $MnO_x$ catalysts followed the same mechanism of CO removal in both plasma catalytic systems despite the different ozone formation processes might occur. In addition, the ozone reductions were similar with the range of 90% as CID reactors larger than 4 cm. This maybe the rate of ozone production which was similar with the rate of ozone decomposition during CID processes.

Besides applied voltage, the power consumption was an important operating parameter for a plasma system. The influence of discharge power on the ozone production by glass/DBD reactors with various

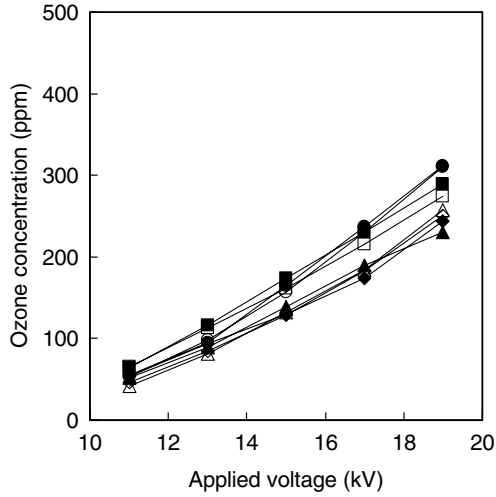


**Fig. 7.** Ozone concentration effluents from CID reactor with different lengths of catalyst-bed. Solid symbol: air without CO. Open symbol: contain 1000 ppm CO. ■, □: 4 cm; ▲, △: 7 cm; ●, ○: 10 cm; ♦, ◇: 13.7 cm.

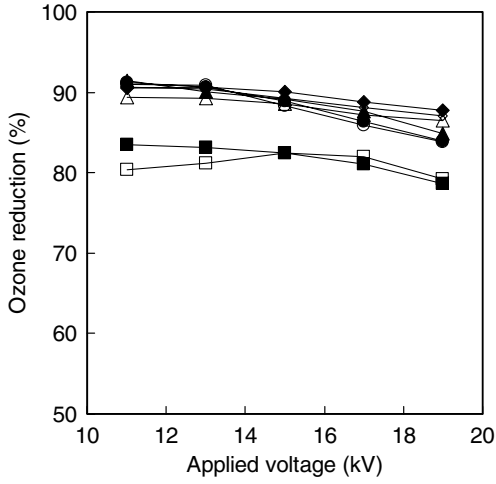


**Fig. 8.** Ozone reduction of CID reactors with different lengths of catalyst-bed as function of applied voltage. Solid symbol: air without CO. Open symbol: contain 1000 ppm CO. ■, □: 4 cm; ▲, △: 7 cm; ●, ○: 10 cm; ♦, ◇: 13.7 cm.

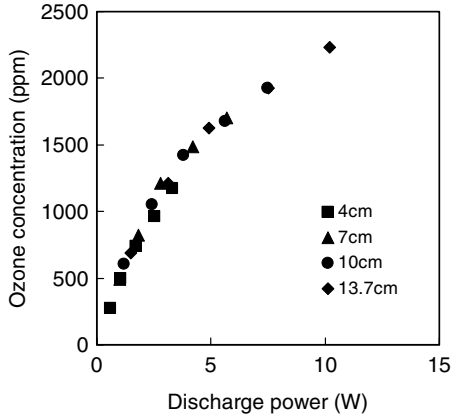


**Fig. 9.** The influence of discharge power on the ozone productions for different lengths of glass/DBD reactors with/without CO.

plasma lengths is shown in Fig. 9. As shown, the ozone concentration was increased with an increasing of discharge power. The curve is similar to the logarithmic function and the similar trend was also reported by Kitayama and Kuzumoto.[18] In addition, the same discharge power applied on ours glass/DBD reactors with different plasma lengths can provide the similar ozone concentration into catalyst-bed. The simplified zone formation model is that the oxidizing species in the gas is primarily formed by the electron impact on molecules directly. Ozone will then mainly be formed by the reactions (1) and (2). Under the lower energy density and lower ozone concentration conditions, such as the discharge power lower than 5 W in our experiment, the ozone formation followed reactions (1) and (2) and increased linearly with the discharge power. However, the dissociation reactions (3) and (4) will become critical under higher energy density and lower ozone concentration condition and complete with reactions (1) and (2). Thus, the curve in Fig. 9 did not increase linearly with the discharge power.

Formation reaction:

$$e + O_2 \rightarrow e + 2O \quad (1)$$

$$O + O_2 + M \rightarrow O_3 + M \quad (2)$$

Dissociation reaction:

$$e + O_3 \rightarrow O + O_2 + e \quad (3)$$

$$O + O_3 \rightarrow 2O_2 \quad (4)$$

The influence of discharge power on the CO removal efficiency for CID and CAD reactors with various catalyst beds is shown in Fig. 10. The three vertical dash lines in Fig. 10 represented 3.3, 5.7 and 7.5 W, respectively. As referred to Fig. 9, the discharge powers of 3.3, 5.7 and 7.5 W can present the CAD reactors with the catalyst-bed lengths of 4, 7 and 10 cm, respectively. Comparing both reactors with the same length of plasma zone and catalyst-bed, the performance of the CAD reactor of CO removal is better than that of the CID reactor if the length of plasma zone and catalyst-bed is smaller than 7 cm. For example, the CO removal efficiency of 4 cm glass/DBD + 4 cm catalyst-bed reactor (CAD reactor) was 72% at 3.3 W (19 kV) whereas that of CID reactor was 51%. When both reactors combined with longer catalyst-bed (> 7 cm), the results show that the CO removal of CID reactor was better than that of CAD reactor at same discharge power. Figure 11 also indicates that a CID reactor is a more economical option than a CAD reactor for CO removal. In addition, the CO removal efficiency of both reactors increased with the decrease of the initial CO concentration.

The CID reactor has the advantage of lower energy consumption at higher CO removal. In addition, the performance of CID did not like that of CAD reactor which would be limited by ozone decomposition. However, the expected large ozone emission is the major concern for the operation of CID reactors. Thus, the best practice is suggested that the

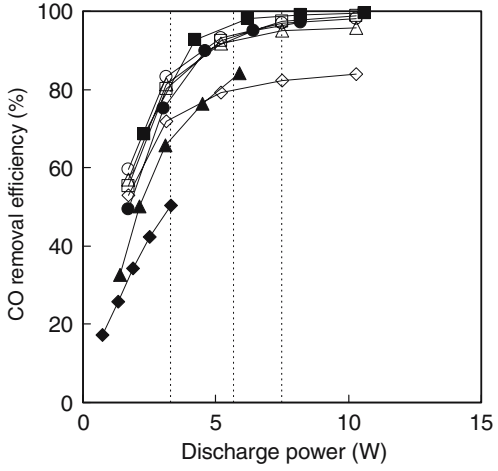


**Fig. 10.** The influence of discharge power on the CO removal of both reactors with different lengths of catalyst-bed. Solid symbol: CID reactor. Open symbol: CAD reactor. ■, □: 4 cm; ▲, △: 7 cm; ●, ○: 10 cm; ♦, ◇: 13.7 cm.

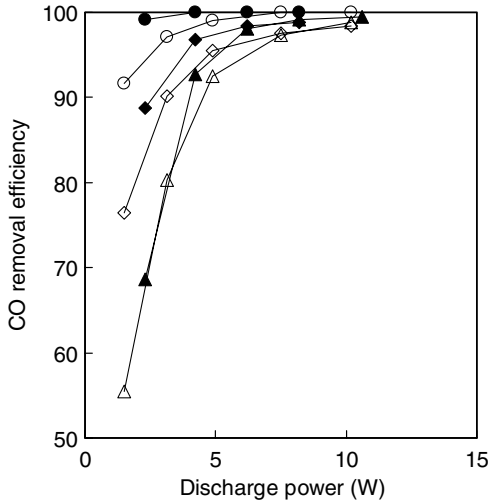


**Fig. 11.** The influence of inlet CO concentrations on both reactors for the CO removal. Solid symbol: CID reactor. Open symbol: CAD reactor. ■, □: 1000 ppm CO; ▲, △: 500 ppm CO; ●, ○: 250 ppm CO.

$MnO_x$ coated pellets placed in the plasma zone of a DBD reactor as a CID reactor to remove CO and then connected to a catalyst-bed to abate ozone emission. The relationship between decomposition efficiency and the length of $MnO_x$ catalyst-bed at varying inlet ozone concentrations is shown in Fig. 12. As shown, the higher inlet ozone concentration requires a longer catalyst-bed to allow elimination completely. For example, Fig. 7 shows that the maximum ozone concentration in CID reactor observed was 312 ppm. Thus, only 7 cm $MnO_x$ catalyst-bed was needed to eliminate the ozone released from the CID reactor.

## 4. CONCLUSIONS

This study successfully demonstrates both catalytic plasma processes for the removal of CO from simulated gas streams. Experimental results indicate that the CO cannot be eliminated by the DBD system without catalysts. When $MnO_x$ catalyst applied to DBD reactors, both CID and CAD reactors could obtain higher CO removal at room temperature without heating. The mechanism of CO removal in both plasma catalytic systems was that the reaction between CO and the active species resulted from ozone decomposition on the $MnO_x$ catalysts. The CO removal of a CID reactor would increase with the decrease of the initial

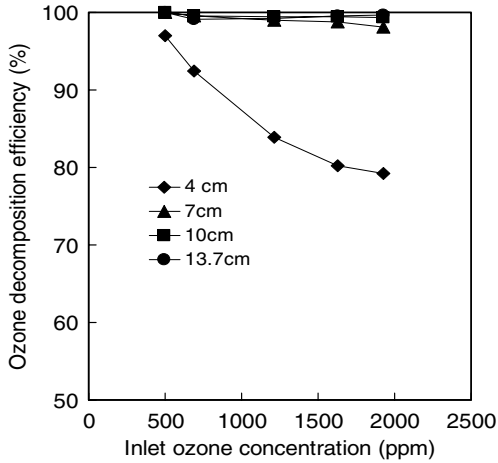


**Fig. 12.** Ozone decomposition of CAD reactors with different lengths of catalyst-bed as function of inlet ozone concentration.

CO concentration and the increase of discharge power and the length of catalyst beds. In addition, the CID reactor has the advantage of lower energy consumption at higher CO removal as compared with the CAD reactor. The CO removal of CAD would be limited by the availability of active species produced from ozone decomposition on the catalyst surface. However, the higher ozone emission is the crucial concern during the CID reactor operation. Thus, the best practice is that the $MnO_x$ coated pellets are placed at the downstream of CID reactor in order to eliminate CO and ozone emission completely.

## ACKNOWLEDGMENTS

The authors would like to thank the National Science Council of the Republic of China for financially supporting this research under Contract No. NSC 91-2211-E-264-004 and NSC 92-2211-E-264-006.

## REFERENCES

1. U. Kogelschatz, *Plasma Chem. Plasma Process.* **23**, 1 (2003).
2. C.-H. Lin and H. Bai, *J. Environ. Eng.-ASCE* **127**, 648 (2001).
3. M. B. Chang and C. C. Chang, *AICHE J.* **43**, 1325 (1997).
4. H. M. Lee and M. B. Chang, *Plasma Chem. Plasma Process.* **23**, 541 (2003).
5. U. Roland, F. Holzer, and F. D. Kopinke, *Catal. Today* **73**, 315 (2002).
6. A. Zang, S. Futamura, and T. Yamamoto, *J. Air Waste Manage. Assoc.* **49**, 1442 (1999).

7. M. A. Malik and X. Z. Jiang, *J. Environ. Sci. (China)* **10**, 276 (1998).
8. H. H. Kim, Y. H. Lee, A. Ogata, and S. Futamura, *Catal. Commun.* **4**, 347 (2003).
9. V. Demidiouk, S. I. Moon, and J. O. Chae, *Catal. Commun*. **4**, 51 (2003).
10. C. Ayrault, J. Barrault, N. Blin-Simiand, F. Jorand, S. Pasquiers, A. Rousseau, and J. M. Tatibouet, *Catal. Today* **89**, 75 (2004).
11. P. Hunter and S. T. Oyama, *Control of Volatile Organic Compound Emissions: Conventional and Emerging Technologies*, John Wiley & Sons, New York, 2000, p. 224.
12. S. Futamura, A. Zang, H. Einaga, and H. Kabashima, *Catal. Today* **72**, 259 (2002).
13. J. O. Chae, V. Demidiouk, M. Yeulash, I. C. Choi, and T. G. Jung, *IEEE Trans. Plasma Sci.* **32**, 493 (2004).
14. Z. Haoa, D. Chengb, Y. Guoc, and Y. Liang, *Appl. Catal. B* **33**, 217 (2001).
15. A. Naydenov, R. Stoyanova, and D. Mehandjiev, *J. Mol. Catal. A*. **98**, 9 (1995).
16. D. Mehandjiev, A. Naydenov, and G. Ivanov, *Appl. Catal. A*. **206**, 13 (2001).
17. H. Einaga and S. Futamura, *J. Catal.* **227**, 304 (2004).
18. J. Kitayama and M. Kuzumoto, *J. Phys. D: Appl. Phys.* **32**, 3032 (1999).